

### 18.3 DIFFRACTION BY A CIRCULAR APERTURE

Let us examine the effect upon the intensity at  $P$  (Fig. 18C) of blocking off the wave by a screen pierced by a small circular aperture as shown in Fig. 18F. If the radius of the hole  $r = OR$  is made equal to the distance  $s_1$  to the outer edge of the first half-period zone,\* the amplitude will be  $A_1$  and this is twice the amplitude due to the unscreened wave. Thus the intensity at  $P$  is 4 times as great as if the screen were absent. When the radius of the hole is increased until it includes the first two zones, the amplitude is  $A_1 - A_2$ , or practically zero. The intensity has actually fallen to almost zero as a result of increasing the size of the hole. A further increase of  $r$  will cause the intensity to pass through maxima and minima each time the number of zones included becomes odd or even.

The same effect is produced by moving the point of observation  $P$  continuously toward or away from the aperture along the perpendicular. This varies the size of the zones, so that if  $P$  is originally at a position such that  $PR - PO$  of Fig. 18F is  $\lambda/2$  (one zone included), moving  $P$  toward the screen will increase this path difference to  $2\lambda/2$  (two zones),  $3\lambda/2$  (three zones), etc. We thus have maxima and minima along the axis of the aperture.

The above considerations give no information about the intensity at points off the axis. A mathematical investigation, which we shall not discuss because of its

\* We are here assuming that the radius of curvature of the wave striking the screen is large, so that distances measured along the chord may be taken as equal to those measured along the arc.

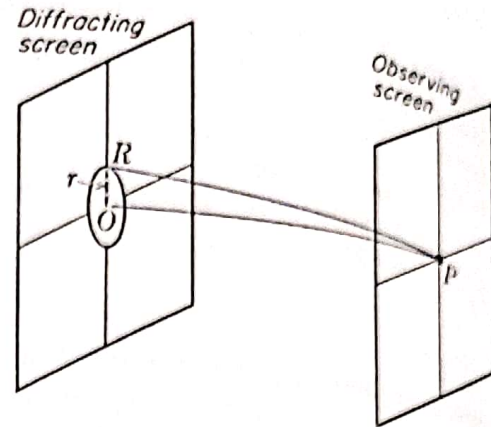


FIGURE 18F  
Geometry for light passing through a circular opening.

complexity,\* shows that  $P$  is surrounded by a system of circular diffraction fringes. Several photographs of these fringes are illustrated in Fig. 18G. These were taken by placing a photographic plate some distance behind circular holes of various sizes, illuminated by monochromatic light from a distant point source. Starting at the upper left of the figures, the holes were of such sizes as to expose one, two, three, etc., zones. The alternation of the center of the pattern from bright to dark illustrates the result obtained above. The large pattern on the right was produced by an aperture containing 71 zones.

#### 18.4 DIFFRACTION BY A CIRCULAR OBSTACLE

When the hole is replaced by a circular disk, Fresnel's method leads to the surprising conclusion that there should be a bright spot in the center of the shadow. For a treatment of this case, it is convenient to start constructing the zones at the edge of the disk. If, in Fig. 18F,  $PR = d$ , the outer edge of the first zone will be  $d + \lambda/2$  from  $P$ , of the second  $d + 2\lambda/2$ , etc. The sum of the series representing the amplitudes from all the zones in this case is, as before, half the amplitude from the first exposed zone. In Fig. 18E it would be obtained by merely omitting the first few vectors. Hence the intensity at  $P$  is practically equal to that produced by the unobstructed wave. This holds only for a point on the axis, however, and off the axis the intensity is small, showing faint concentric rings. In Fig. 18H(a) and (b), which shows photographs of the bright spot, these rings are unduly strengthened relative to the spot by overexposure. In (c) the source, instead of being a point, was a photographic negative of a portrait of Woodrow Wilson on a transparent plate, illuminated from behind. The disk acts like a rather crude lens in forming an image, since for every point in the object there is a corresponding bright spot in the image.

The complete investigation of diffraction by a circular obstacle shows that, besides the spot and faint rings in the shadow, there are bright circular fringes bordering the outside of the shadow. These are similar in origin to the diffraction fringes from a straight edge to be investigated in Sec. 18.11.

\* See T. Preston, "Theory of Light," 5th ed., pp. 324-327, The Macmillan Company, New York, 1928.

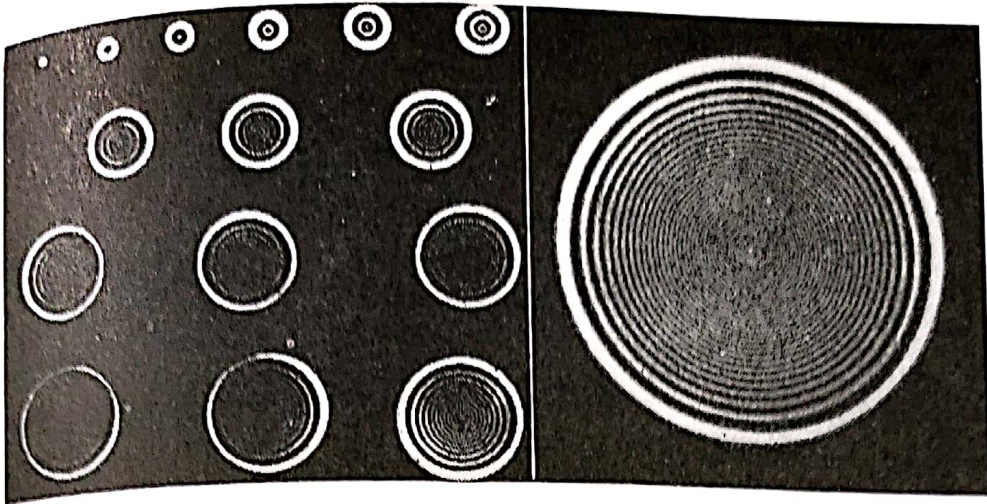


FIGURE 18G  
Diffraction of light by small circular openings. (Courtesy of Hufford.)

The bright spot in the center of the shadow of a 1-cent piece can be seen by examining the region of the shadow produced by an arc light several meters away, preferably using a magnifying glass. The spot is very tiny in this case and difficult to find. It is easier to see with a smaller object, such as a bearing ball.

### 18.5 ZONE PLATE

This is a special screen designed to block off the light from every other half-period zone. The result is to remove either all the positive terms in Eq. (18d) or all the negative terms. In either case the amplitude at  $P$  (Fig. 18C) will be increased to many times its value in the above cases. A zone plate can easily be made in practice by drawing concentric circles on white paper, with radii proportional to the square roots of whole numbers (see Fig. 18I). Every other zone is then blackened, and the result is photographed on a reduced scale. The negative, when held in the light from a distant point source, produces a large intensity at a point on its axis at a distance corresponding

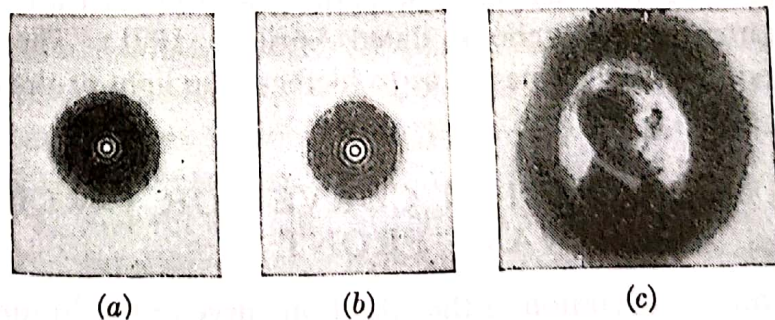


FIGURE 18H  
Diffraction by a circular obstacle: (a) and (b) point source; (c) a negative of Woodrow Wilson as a source. (Courtesy of Hufford.)

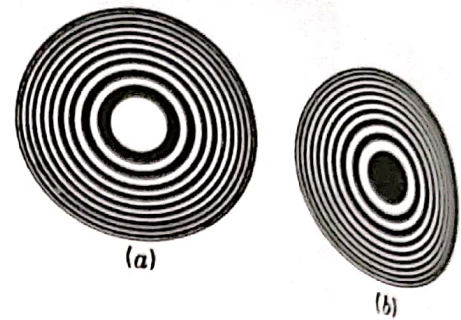


FIGURE 18I  
Zone plates.

to the size of the zones and the wavelength of the light used. The relation between these quantities is contained in Eq. (18b), which for the present purpose may be written

$$m \frac{\lambda}{2} = \frac{s_m^2}{2} \left( \frac{1}{a} + \frac{1}{b} \right) \quad (18h)$$

Hence we see that, for given  $a$ ,  $b$ , and  $\lambda$ , the zones must have  $s_m \approx \sqrt{m}$ .

The bright spot produced by a zone plate is so intense that the plate acts much like a lens. Thus suppose that the first 10 odd zones are exposed, as in the zone plate of Fig. 18I(a). This leaves the amplitudes  $A_1, A_3, A_5, \dots, A_{19}$  (see Fig. 18E), the sum of which is nearly 10 times  $A_1$ . The whole wave front gives  $\frac{1}{2}A_1$ , so that, using only 10 exposed zones, we obtain an amplitude at  $P$  which is 20 times as great as when the plate is removed. The intensity is therefore 400 times as great. If the odd zones are covered, the amplitudes  $A_2, A_4, A_6, \dots$  will give the same effect. The object and image distances obey the ordinary lens formula, since, by Eq. (18h),

$$\frac{1}{a} + \frac{1}{b} = \frac{m\lambda}{s_m^2} = \frac{1}{f}$$

the focal length  $f$  being the value of  $b$  for  $a = \infty$ , namely,

$$f = \frac{s_m^2}{m\lambda} = \frac{s_1^2}{\lambda} \quad (18i)$$

There are also fainter images corresponding to focal lengths  $f/3, f/5, f/7, \dots$ , because at these distances each zone of the plate includes 3, 5, 7, ... Fresnel zones. When it includes three, for example, the effects of two of them cancel but that of the third is left over.

Apparently the zone plate was invented by Lord Rayleigh as evidenced by an entry in his notebook, dated April 11, 1871: "The experiment of blocking out the odd Huygens zones so as to increase the light at the center succeeded very well..."

### 18.6 VIBRATION CURVE FOR CIRCULAR DIVISION OF THE WAVE FRONT

Our consideration of the vibration curve in the Fraunhofer diffraction by a single slit (Sec. 15.4) was based upon the division of the plane wave front into infinitesimal elements of area which were actually strips of infinitesimal width parallel to the length of the diffracting slit. The vectors representing the contributions to the amplitude

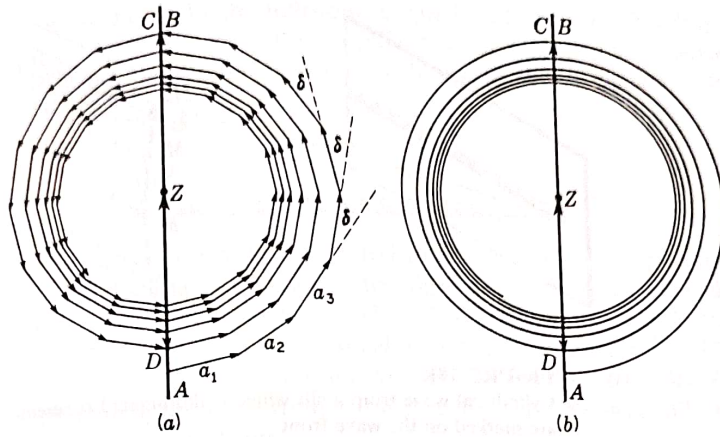


FIGURE 18J  
Vibration spiral for Fresnel half-period zones of a circular opening.

from these elements were found to give an arc of a circle. This so-called *strip division* of the wave front is appropriate when the source of light is a narrow slit and the diffracting aperture rectangular. The strip division of a divergent wave front from such a source will be discussed below (Sec. 18.8). The method of dividing the spherical wave from a point source appropriate to any case of diffraction by circular apertures or obstacles involves infinitesimal circular zones.

Let us consider first the amplitude diagram when the first half-period zone is divided into eight subzones, each constructed in a manner similar to that used for the half-period zones themselves. We make these subzones by drawing circles on the wave front (Fig. 18C) which are distant

$$b + \frac{1}{8} \frac{\lambda}{2}, \quad b + \frac{2}{8} \frac{\lambda}{2}, \quad \dots, \quad b + \frac{\lambda}{2}$$

from  $P$ . The light arriving at  $P$  from various points in the first subzone will not vary in phase by more than  $\pi/8$ . The resultant of these may be represented by the vector  $a_1$  in Fig. 18J(a). To this is now added  $a_2$ , the resultant amplitude due to the second subzone, then  $a_3$  due to the third subzone, etc. The magnitudes of these vectors will decrease very slowly as a result of the obliquity factor. The phase difference  $\delta$  between each successive one will be constant and equal to  $\pi/8$ . Addition of all eight subzones yields the vector  $AB$  as the resultant amplitude from the first half-period zone. Continuing this process of subzoning to the second half-period zone, we find  $CD$  as the resultant for this zone, and  $AD$  as that for the sum of the first two zones. These vectors correspond to those of Fig. 18E. Succeeding half-period zones give the rest of the figure, as shown.

The transition to the vibration curve of Fig. 18J(b) results from increasing indefinitely the number of subzones in a given half-period zone. The curve is now a *vibration spiral*, eventually approaching  $Z$  when the half-period zones cover the whole

## URES AND OBSTACLES WITH

ion of the diffracting screen, instead of h  
edges like those of a slit or wire, it is po  
a point. The slit is set parallel to these e  
produced by each element of its length are  
siderable gain of intensity is achieved ther  
s possible to regard the wave front as cyli  
at to produce such a cylindrical envelope  
is points on the slit these must emit *col*  
ly be true. Nevertheless, when intensities  
mission, the resulting pattern is the same



NOTE 7 PRO  
L CAMERA

2020

by a coherent cylindrical wave. In the following treatment of problems involving straight edges, we shall therefore make the simplification of assuming the source slit to be illuminated by a parallel monochromatic beam, so that it emits a truly cylindrical wave.

### 18.8 STRIP DIVISION OF THE WAVE FRONT

The appropriate method of constructing half-period elements on a cylindrical wave front consists in dividing the latter into strips, the edges of which are successively one-half wavelength farther from the point  $P$  (Fig. 18K). Thus the points  $M_0, M_1, M_2, \dots$  on the circular section of the cylindrical wave are at distances  $b, b + \lambda/2, b + 2\lambda/2, \dots$  from  $P$ .  $M_0$  is on the straight line  $SP$ . The half-period strips  $M_0M_1, M_1M_2, \dots$  now stretch along the wave front parallel to the slit. We may call this procedure *strip division* of the wave front.

In the Fresnel zones obtained by circular division, the areas of the zones were very nearly equal. With the present type of division this is by no means true. The areas of the *half-period strips* are proportional to their widths, and these decrease rapidly as we go out along the wave front from  $M_0$ . Since this effect is much more pronounced than any variation of the obliquity factor, the latter need not be considered.

The amplitude diagram of Fig. 18L(a) is obtained by dividing the strips into substrips in a manner analogous to that described in Sec. 18.6 for circular zones. Dividing the first strip above  $M_0$  into nine parts, we find that the nine amplitude vectors from the substrips extend from  $O$  to  $B$ , giving a resultant  $A_1 = OB$ , for the first half-period strip. The second half-period strip similarly gives those between  $B$  and  $C$ , with a resultant  $A_2 = BC$ . Since the amplitudes now decrease rapidly,  $A_2$  is considerably smaller than  $A_1$ , and their difference in phase is appreciably greater than  $\pi$ . A repetition of this process of subdivision for the succeeding strips on the upper half of the wave gives the more complete diagram of Fig. 18L(b). Here the vectors are spiraling in toward  $Z$ , so that the resultant for all half-period strips above the pole  $M_0$  becomes  $OZ$ .

### 18.9 VIBRATION CURVE FOR STRIP DIVISION. CORNU'S SPIRAL

When we go over to elementary strips of infinitesimal width, we obtain the vibration curve as a smooth spiral, part of which is shown in Fig. 18M. The complete curve representing the whole wave front would be carried through many more turns, ending at the points  $Z$  and  $Z'$ . Only the part from  $O$  to  $Z$  was considered above. The lower half,  $Z'O$ , arises from the contributions from the half-period strips below  $M_0$ .

This curve, called *Cornu's\* spiral*, is characterized by the fact that the angle  $\delta$

\* M. A. Cornu (1841–1902). Professor of experimental physics at the École Polytechnique, Paris.

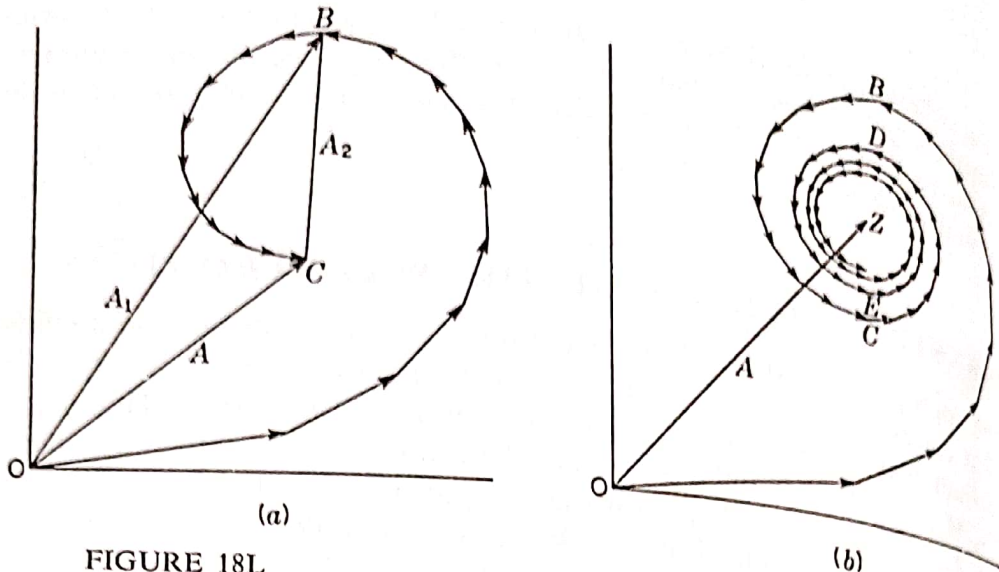


FIGURE 18L  
Amplitude diagrams for the formation of Cornu's spiral.

it makes with the  $x$  axis is proportional to the *square* of the distance  $v$  along the curve from the origin. Remembering that, in a vibration curve,  $\delta$  represents the phase lag in the light from any element of the wave front, we obtain this definition of the curve by using Eq. (18a) for the path difference, as follows:

$$\delta = \frac{2\pi}{\lambda} \Delta = \frac{\pi(a + b)}{ab\lambda} s^2 = \frac{\pi}{2} v^2 \quad (18j)$$

Here we have introduced a new variable for use in plotting Cornu's spiral, namely

$$v = s \sqrt{\frac{2(a + b)}{ab\lambda}} \quad (18k)$$

$v$  is defined in such a way as to make it dimensionless, so that the same curve may be used for any problem, regardless of the particular values of  $a$ ,  $b$ , and  $\lambda$ .

### 8.10 FRESNEL'S INTEGRALS

The  $x$  and  $y$  coordinates of Cornu's spiral can be expressed quantitatively by two integrals, and a knowledge of them will permit accurate plotting and calculations. They are derived most simply as follows. Since the phase difference  $\delta$  is the angle determining the slope of the curve at any point (see Fig. 18M), the changes in the coordinates for a given small displacement  $dv$  along the spiral are given by

$$dx = dv \cos \delta = \cos \frac{\pi v^2}{2} dv \quad dy = dv \sin \delta = \sin \frac{\pi v^2}{2} dv$$



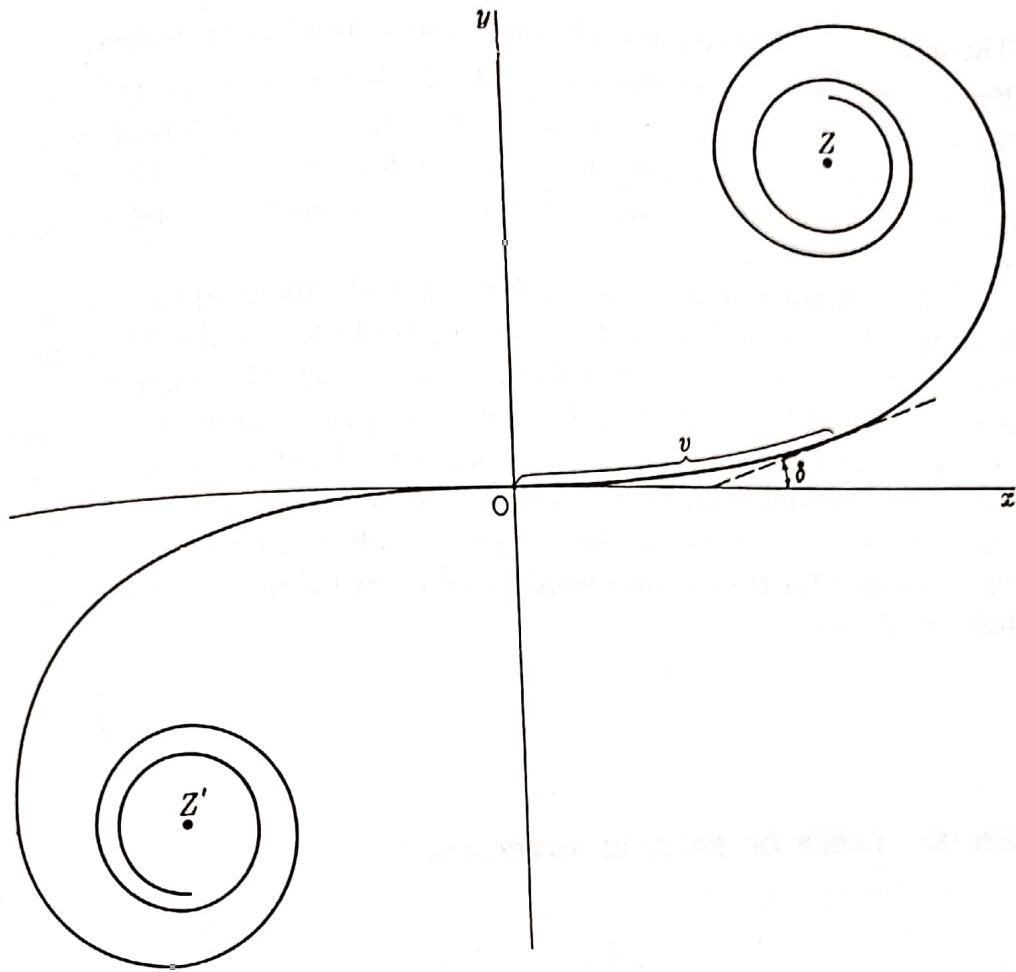


FIGURE 18M  
Cornu's spiral drawn to include five half-period zones on either side of the pole.

where the value of  $\delta$  from Eq. (18j) has been introduced. Thus the coordinates of any point  $(x,y)$  on Cornu's spiral become

$$x = \int_0^v \cos \frac{\pi v^2}{2} dv \quad (18l)$$

$$y = \int_0^v \sin \frac{\pi v^2}{2} dv \quad (18m)$$

These are known as *Fresnel's integrals*. They cannot be integrated in closed form but yield infinite series which may be evaluated in several ways.\* Although the actual evaluation is too complicated to be given here, we have included a table of the numerical values of the integrals (Table 18A). In Sec. 18.14 the method of using them in accurate computations of diffraction patterns is explained.

Let us first examine some features of the quantitative Cornu's spiral of Fig. 18N, which is a plot of the two Fresnel integrals. The coordinates of any point on the curve give their values for a particular upper limit  $v$  in Eqs. (18l) and (18m).

\* For the methods of evaluating Fresnel's integrals, see R. W. Wood, "Physical Optics," 2d ed., p. 247, The Macmillan Company, New York, 1921; reprinted (paperback) by Dover Publications, Inc., New York, 1968.

The scale of  $v$  is marked directly on the curve and has equal divisions along its length. Particularly useful to remember are the positions of the points  $v = 1, \sqrt{2}$ , and 2 on the curve. They represent one-half, one, and two half-period strips, respectively, as can be verified by computing the corresponding values of  $\delta$  from Eq. (18j). More important, however, are the coordinates of the end points  $Z'$  and  $Z$ . They are  $(-\frac{1}{2}, -\frac{1}{2})$  and  $(\frac{1}{2}, \frac{1}{2})$ , respectively.

As with any vibration curve, the amplitude due to any given portion of the wave front may be obtained by finding the length of the chord of the appropriate segment of the curve. The square of this length then gives the intensity. Thus the Cornu's spiral of Fig. 18N can be used for the graphical solution of diffraction problems, as will be illustrated below. It is to be noted at the start, however, that the numerical values of intensities computed in this way are *relative to a value of 2 for the unobstructed wave*. Thus, if  $A$  represents any amplitude obtained from the plot, the intensity  $I$ , expressed as a fraction of that which would exist if no screen were present, which we shall call  $I_0$ , is

$$\frac{I}{I_0} = \frac{1}{2}A^2 \quad (18n)$$

Table 18A TABLE OF FRESNEL INTEGRALS

$v$	$x$	$y$	$v$	$x$	$y$	$v$	$x$	$y$
0.00	0.0000	0.0000	3.00	0.6058	0.4963	5.50	0.4784	0.5537
0.10	0.1000	0.0005	3.10	0.5616	0.5818	5.55	0.4456	0.5181
0.20	0.1999	0.0042	3.20	0.4664	0.5933	5.60	0.4517	0.4700
0.30	0.2994	0.0141	3.30	0.4058	0.5192	5.65	0.4926	0.4441
0.40	0.3975	0.0334	3.40	0.4385	0.4296	5.70	0.5385	0.4595
0.50	0.4923	0.0647	3.50	0.5326	0.4152	5.75	0.5551	0.5049
0.60	0.5811	0.1105	3.60	0.5880	0.4923	5.80	0.5298	0.5461
0.70	0.6597	0.1721	3.70	0.5420	0.5750	5.85	0.4819	0.5513
0.80	0.7230	0.2493	3.80	0.4481	0.5656	5.90	0.4486	0.5163
0.90	0.7648	0.3398	3.90	0.4223	0.4752	5.95	0.4566	0.4688
1.00	0.7799	0.4383	4.00	0.4984	0.4204	6.00	0.4995	0.4470
1.10	0.7638	0.5365	4.10	0.5738	0.4758	6.05	0.5424	0.4689
1.20	0.7154	0.6234	4.20	0.5418	0.5633	6.10	0.5495	0.5165
1.30	0.6386	0.6863	4.30	0.4494	0.5540	6.15	0.5146	0.5496
1.40	0.5431	0.7135	4.40	0.4383	0.4622	6.20	0.4676	0.5398
1.50	0.4453	0.6975	4.50	0.5261	0.4342	6.25	0.4493	0.4954
1.60	0.3655	0.6389	4.60	0.5673	0.5162	6.30	0.4760	0.4555
1.70	0.3238	0.5492	4.70	0.4914	0.5672	6.35	0.5240	0.4560
1.80	0.3336	0.4508	4.80	0.4338	0.4968	6.40	0.5496	0.4965
1.90	0.3944	0.3734	4.90	0.5002	0.4350	6.45	0.5292	0.5398
2.00	0.4882	0.3434	5.00	0.5637	0.4992	6.50	0.4816	0.5454
2.10	0.5815	0.3743	5.05	0.5450	0.5442	6.55	0.4520	0.5078
2.20	0.6363	0.4557	5.10	0.4998	0.5624	6.60	0.4690	0.4631
2.30	0.6266	0.5531	5.15	0.4553	0.5427	6.65	0.5161	0.4549
2.40	0.5550	0.6197	5.20	0.4389	0.4969	6.70	0.5467	0.4915
2.50	0.4574	0.6192	5.25	0.4610	0.4536	6.75	0.5302	0.5362
2.60	0.3890	0.5500	5.30	0.5078	0.4405	6.80	0.4831	0.5436
2.70	0.3925	0.4529	5.35	0.5490	0.4662	6.85	0.4539	0.5060
2.80	0.4675	0.3915	5.40	0.5573	0.5140	6.90	0.4732	0.4624
2.90	0.5624	0.4101	5.45	0.5269	0.5519	6.95	0.5207	0.4591

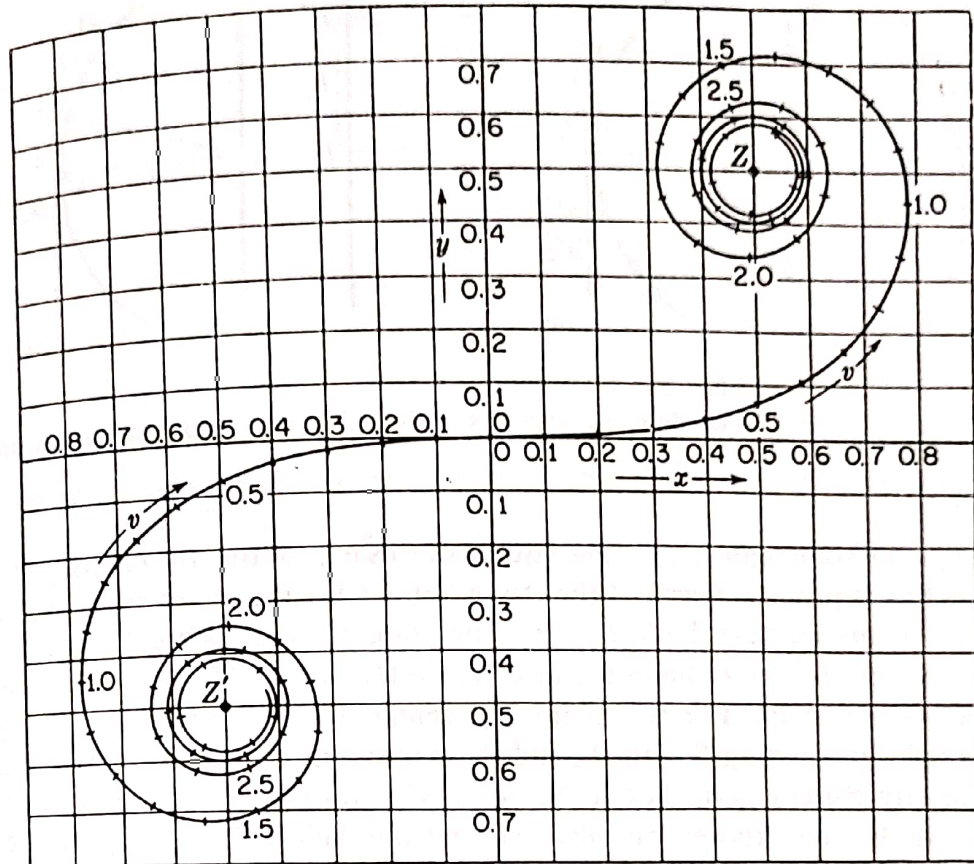


FIGURE 18N  
Cornu's spiral; a plot of the Fresnel integrals.

To verify this statement, we note that according to the discussion of Sec. 18.8 a vector drawn from  $O$  to  $Z$  gives the amplitude due to the upper half of the wave. Similarly, one from  $Z'$  to  $O$  gives that due to the lower half. Each of these has a magnitude  $1/\sqrt{2}$ , so that when they are added and the sum is squared to obtain the intensity due to the whole wave, we find that  $I_0 = 2$ , with the conventional scale of coordinates used in Fig. 18N.\*

### 18.11 THE STRAIGHT EDGE

The investigation of the diffraction by a single screen with a straight edge is perhaps the simplest application of Cornu's spiral. Figure 18O(a) represents a section of such a screen, having its edge parallel to the slit  $S$ . In this figure the half-period strip corresponding to the point  $P$  being situated on the edge of the geometrical shadow are marked off on the wave front. To find the intensity at  $P$ , we note that since the upper half of the wave is effective, the amplitude is a straight line joining  $O$  and  $Z$

\* It will be noticed that the phase of the resultant wave is  $45^\circ$ , or one-eighth period behind that of the wave coming from the center of the zone system (the Huygen wavelet reaching  $P$  from  $M_0$  in Fig. 18K). A similar phase discrepancy, this time one-quarter period, occurs in the treatment of circular zones in Sec. 18.6. For discussion of the phase discrepancy in Cornu's spiral, see R. W. Ditchburn, "Light" p. 214, Interscience Publishers, Inc., New York, 1953; 2d ed (paperback), 1963.

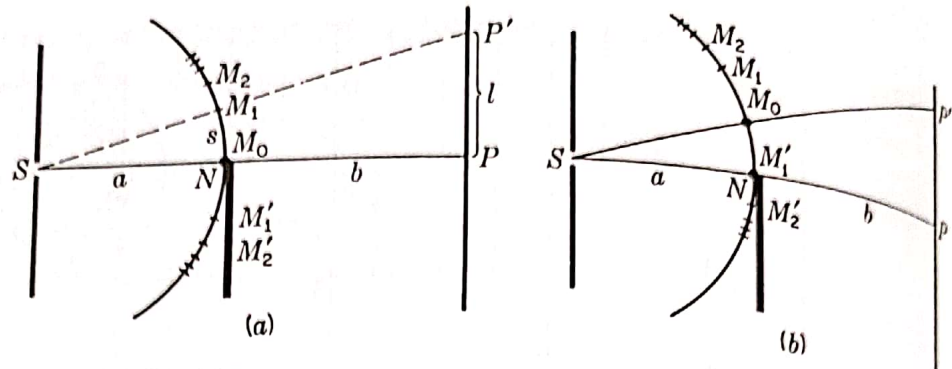


FIGURE 18O

Two different positions of the half-period strips relative to a straight edge  $N$ .

(Fig. 18P) of length  $1/\sqrt{2}$ . The square of this is  $\frac{1}{2}$ , so that the intensity at the edge of the shadow is just *one-fourth* of that found above for the unobstructed wave.

Consider next the intensity at the point  $P'$  [Fig. 18O(a)] at a distance  $l$  above  $P$ . To be specific, let  $P'$  lie in the direction  $SM_1$ , where  $M_1$  is the upper edge of the first half-period strip. For this point, the center  $M_0$  of the half-period strips lies on the straight line joining  $S$  with  $P'$ , and the figure must be reconstructed as in Fig. 18O(b). The straight edge now lies at the point  $M'_1$ , so that not only all the half-period strips above  $M_0$  are exposed but also the first one below  $M_0$ . The resultant amplitude  $A$  is therefore represented on the spiral of Fig. 18P by a straight line joining  $B'$  and  $Z$ . This amplitude is more than twice that at  $P$ , and the intensity  $A^2$  more than 4 times as great.

Starting with the point of observation  $P$  at the edge of the geometrical shadow (Fig. 18O), where the amplitude is given by  $OZ$ , if we move the point steadily upward, the tail of the amplitude vector moves to the left along the spiral, while its head remains fixed at  $Z$ . The amplitude will evidently go through a maximum at  $b'$ , a minimum at  $c'$ , another maximum at  $d'$ , etc., approaching finally the value  $Z'Z$  for the unobstructed wave. If we go downward from  $P$ , into the geometrical shadow, the tail of the vector moves to the right from  $O$ , and the amplitude will decrease steadily, approaching zero.

To obtain quantitative values of the intensities from Cornu's spiral, it is only necessary to measure the length  $A$  for various values of  $v$ . The square of  $A$  gives the intensity. Plots of the amplitude and the intensity against  $v$  are shown in Figs. 18Q(a) and (b), respectively. It will be seen that at the point  $O$ , which corresponds to the edge of the geometrical shadow, the intensity has fallen to one-fourth that for large negative values of  $v$ , where it approaches the value for the unobstructed wave. The other letters correspond with points similarly labeled on the spiral,  $B', C', D', \dots$  representing the exposure of one, two, three, etc., half-period strips below  $M_0$ . The maxima and minima of these *diffraction fringes* occur a little before these points are reached. For instance, the first maximum at  $b'$  is given when the amplitude vector  $A$  has the position shown in Fig. 18P. Photographs of the diffraction pattern from a straight edge are shown in Fig. 18R(a) and (b). Pattern (a) was taken with visible light from a mercury arc, and (b) with X rays,  $\lambda = 8.33 \text{ \AA}$ . Figure 18R(c) is a density trace of the photograph (a), directly above, and was made with a microphotometer.

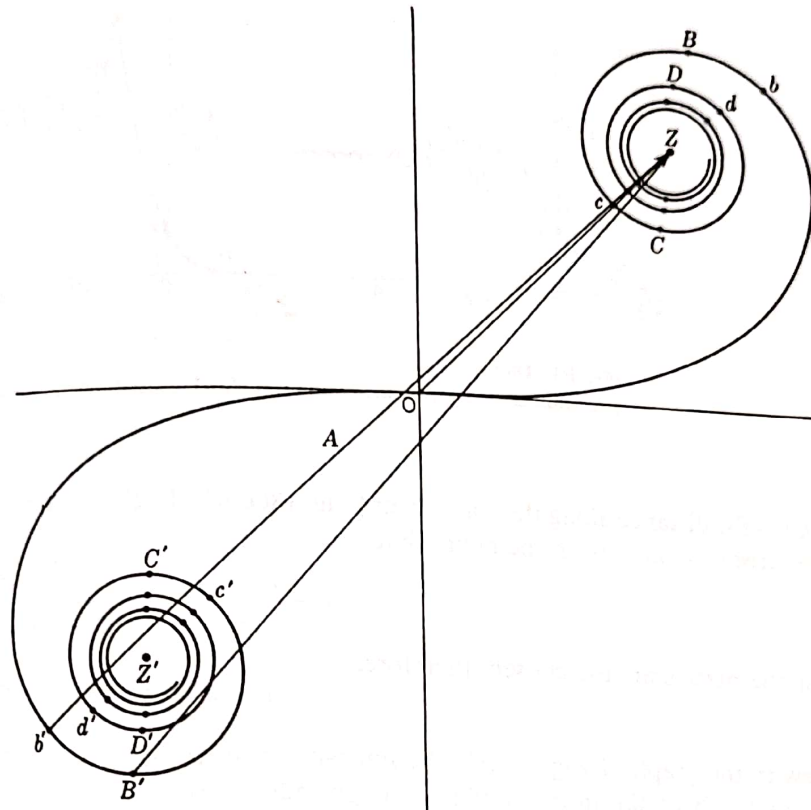


FIGURE 18P  
Cornu's spiral, showing resultants for a straight-edge diffraction pattern.

Perhaps the most common observation of the straight-edge pattern, and certainly a very striking one, occurs in viewing a distant street lamp through rain-spattered spectacles. The edge of each drop as it stands on the glass acts like a prism, and refracts into the pupil of the eye rays which otherwise would not enter it. Beyond the edge the field is therefore dark, but the crude outline of the drop is seen as an irregular bright patch bordered by intense diffraction fringes such as those shown in Fig. 18R. The fringes are very clear, and a surprising number can be seen, presumably because of the achromatizing effect of the refraction.

### 18.12 RECTILINEAR PROPAGATION OF LIGHT

When we investigate the *scale* of the above pattern for a particular case, the reason for the apparently rectilinear propagation of light becomes clear. Let us suppose that in a particular case  $a = b = 100$  cm, and  $\lambda = 5000 \text{ \AA}$ . From Eq. (18k), we then have

$$s = v \sqrt{\frac{ab\lambda}{2(a+b)}} = 0.0354v \quad \text{cm}$$

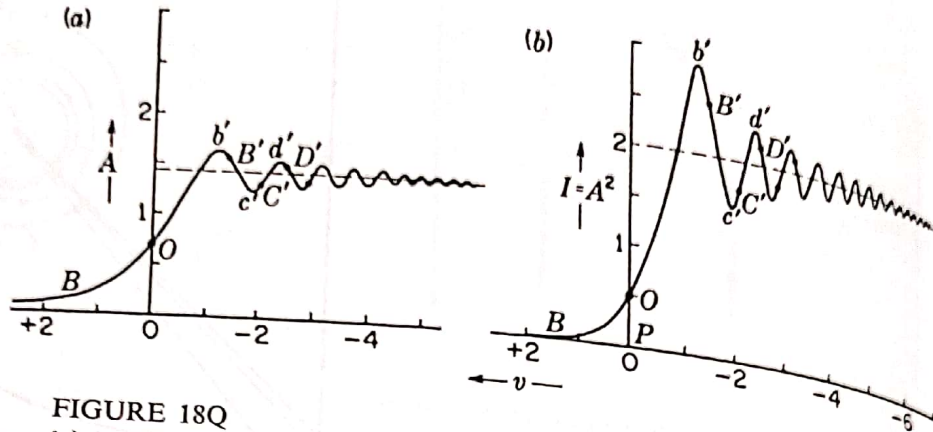


FIGURE 18Q  
 (a) Amplitude and (b) intensity contours for Fresnel diffraction at a straight edge.

This is the distance along the wave front [Fig. 18O(a)]. To change it to distances  $l$  on the screen, we note from the figure that

$$l = \frac{a+b}{a} s = v \sqrt{\frac{b\lambda(a+b)}{2a}} \quad (180)$$

For the particular case chosen, therefore,

$$l = 2s = 0.0708v \quad \text{cm}$$

Now in the graph of Fig. 18Q(b) the intensity at the point  $v = +2$  is only 0.025 or one-eighth of the intensity if the straight edge were absent. This point has  $l = 0.142$  cm, and therefore lies only 1.42 mm inside the edge of the geometrical shadow.

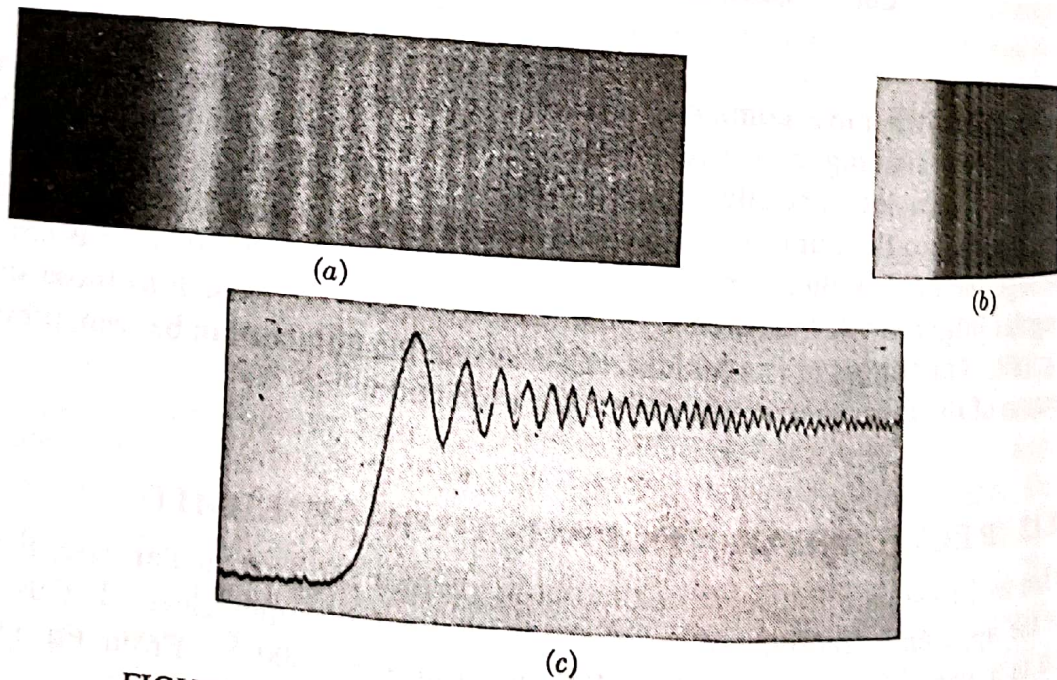


FIGURE 18R  
 Straight-edge diffraction patterns photographed with (a) visible light of wavelength 4300 Å and (b) X rays of wavelength 8.33 Å. (c) Microphotometer trace of (a).

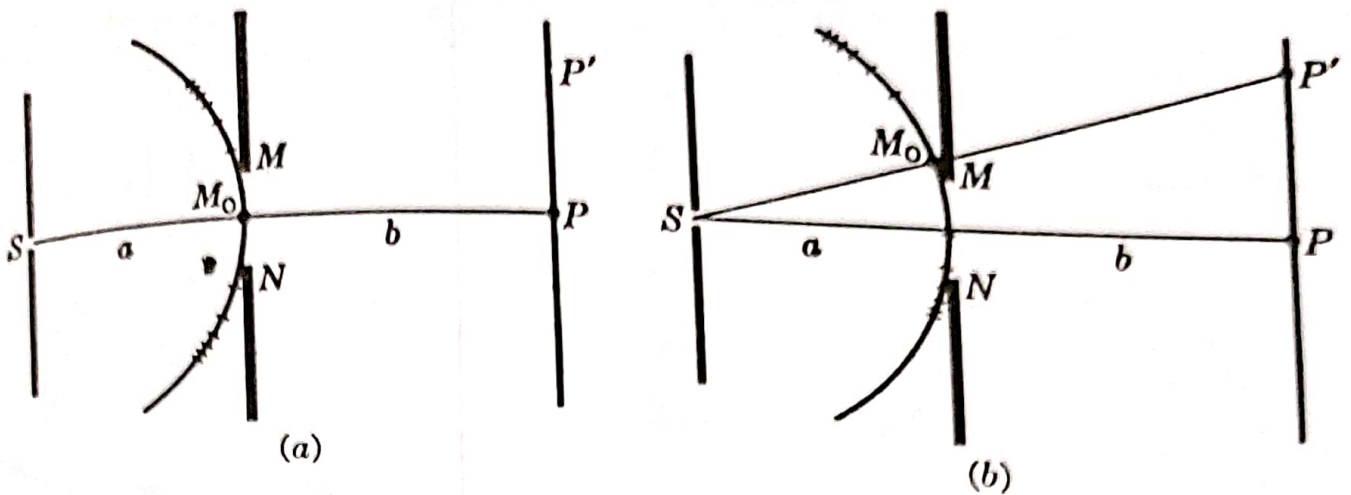


FIGURE 18S  
Division of the wave front for Fresnel diffraction by a single slit.

The part of the screen below this will lie in practically complete darkness, and this must be due to the destructive interference of the secondary wavelets arriving here from the upper part of the wave.

### 18.13 SINGLE SLIT

We next consider the Fresnel diffraction of a single slit with sides parallel to a narrow source slit  $S$  [Fig. 18S(a)]. By the use of Cornu's spiral we wish to determine the distribution of the light on the screen  $PP'$ . With the slit 100  $\mu$ m wide and the source slit 100  $\mu$ m wide, the slit acts like a straight edge to the source slit.

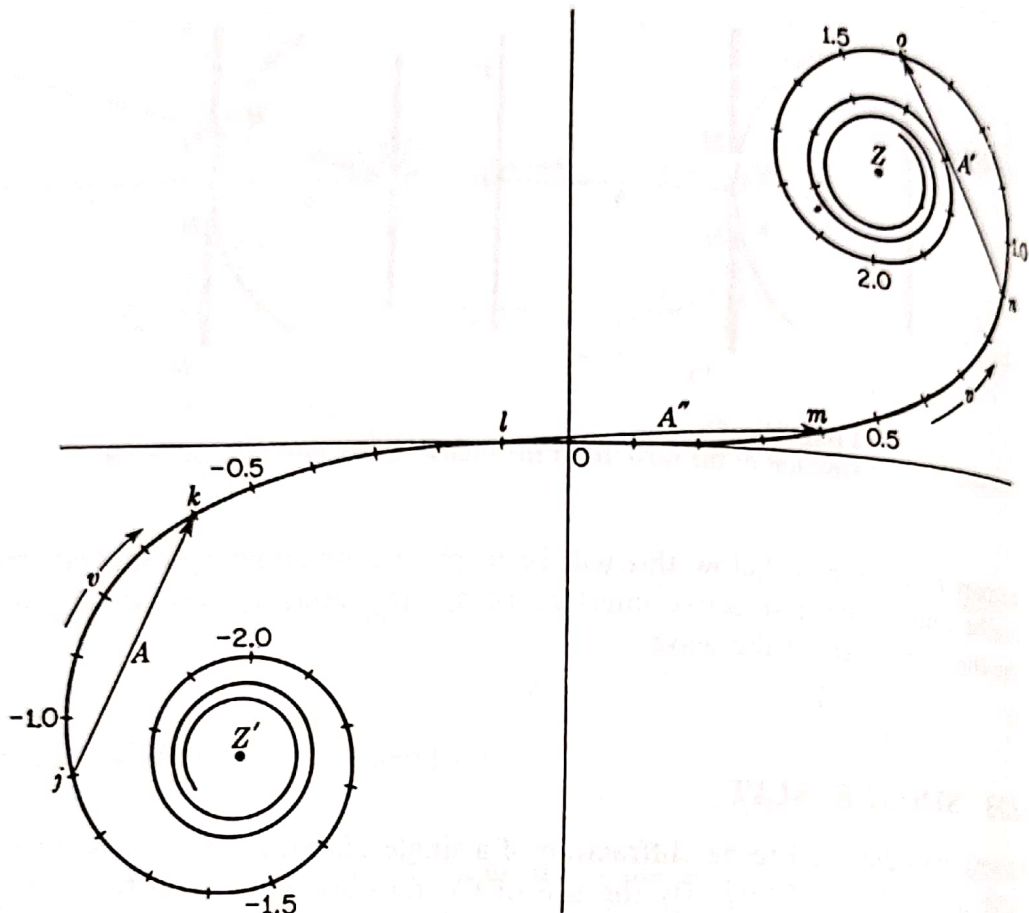


FIGURE 18T

Cornu's spiral, showing the chords of arcs of equal lengths  $\Delta v$ .

student may make a straight scale marked off in units of  $v$  to tenths, and measure the chords on an accurate plot such as Fig. 18N, using the scale of  $v$  on the spiral to obtain the constant length  $\Delta v$  of the arc. The results should then be tabulated in three columns, giving  $v$ ,  $A$ , and  $A^2$ . The value of  $v$  to be entered is that for the *central* point of the arc whose chord  $A$  is being measured. For example, if the interval from  $v = 0.9$  to  $v = 1.4$  measured (Fig. 18T), the average value  $v = 1.15$  is tabulated against  $A = 0.43$ .

Photographs of a number of Fresnel diffraction patterns for single slits of different widths are shown in Fig. 18U with the corresponding intensity curves beside them. These curves have been plotted by the use of Cornu's spiral. It is of interest to note in these diagrams the indicated positions of the edges of the geometrical shadow of the slit (indicated on the  $v$  axis). Very little light falls outside these points. For a very narrow slit like the first of these where  $\Delta v = 1.5$ , the pattern greatly resembles the Fraunhofer diffraction pattern for a single slit. The essential difference between the two (compare Fig. 15D) is that here the minima do not come quite to zero except at infinitely large  $v$ . The small single-slit pattern at the top was taken with X rays of wavelength  $8.33 \text{ \AA}$ , while the rest were taken with visible light of wavelength  $358 \text{ \AA}$ . As the slit becomes wider, the fringes go through very rapid changes, approach-



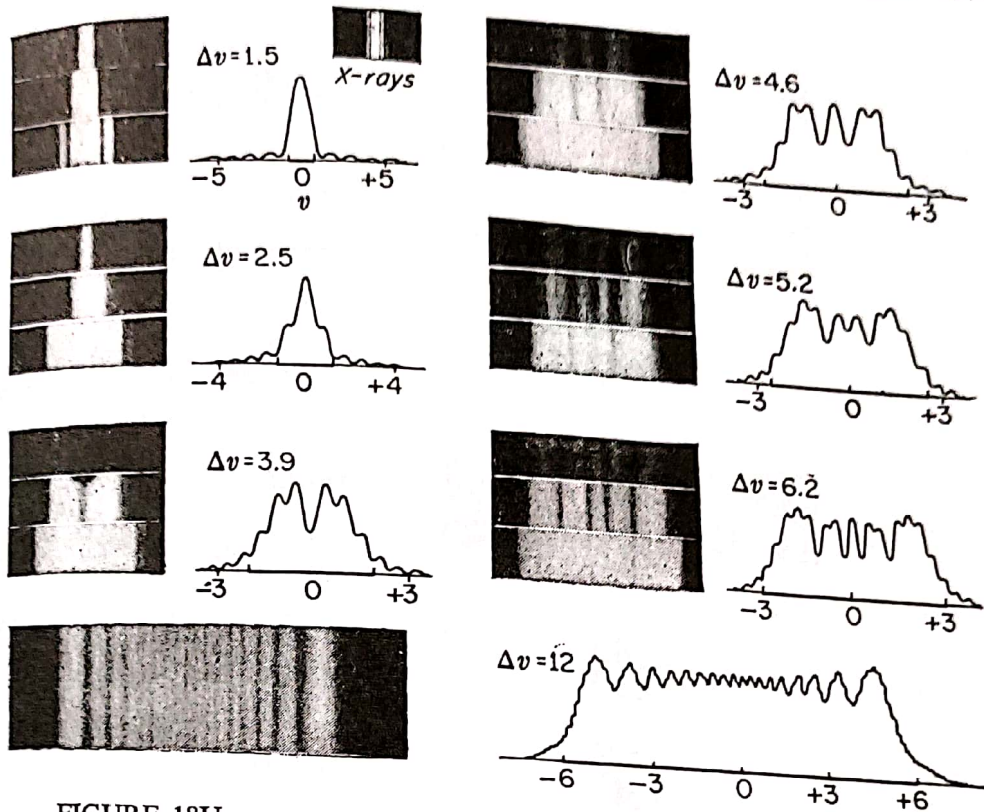


FIGURE 18U  
Fresnel diffraction of visible light by single slits of different widths. (X-ray pattern courtesy of Kellstrom, University of Uppsala, Uppsala, Sweden.)

ing for a wide slit the general appearance of two opposed straight-edge diffraction patterns. The small closely spaced fringes superimposed on the main fringes at the outer edges of the last figure are clearly seen in the original photograph and may be detected in the reproduction.

### 18.14 USE OF FRESNEL'S INTEGRALS IN SOLVING DIFFRACTION PROBLEMS

The tabulated values of Fresnel's integrals in Table 18A can be used for higher accuracy than that obtainable with the plotted spiral. For an interval  $\Delta v = 0.5$ , for example, the two values of  $x$  at the ends of this interval are read from the table and subtracted algebraically to obtain  $\Delta x$ , the horizontal component of the amplitude. The corresponding two values of  $y$  are also subtracted to obtain  $\Delta y$ , its vertical component. The relative intensity will then be obtained by adding the squares of these quantities, since

$$I \approx A^2 = (\Delta x)^2 + (\Delta y)^2 \quad (18p)$$

The method is accurate but may be tedious, especially if good interpolations are to be made in certain parts of Table 18A. Some problems, such as that of the straight edge,

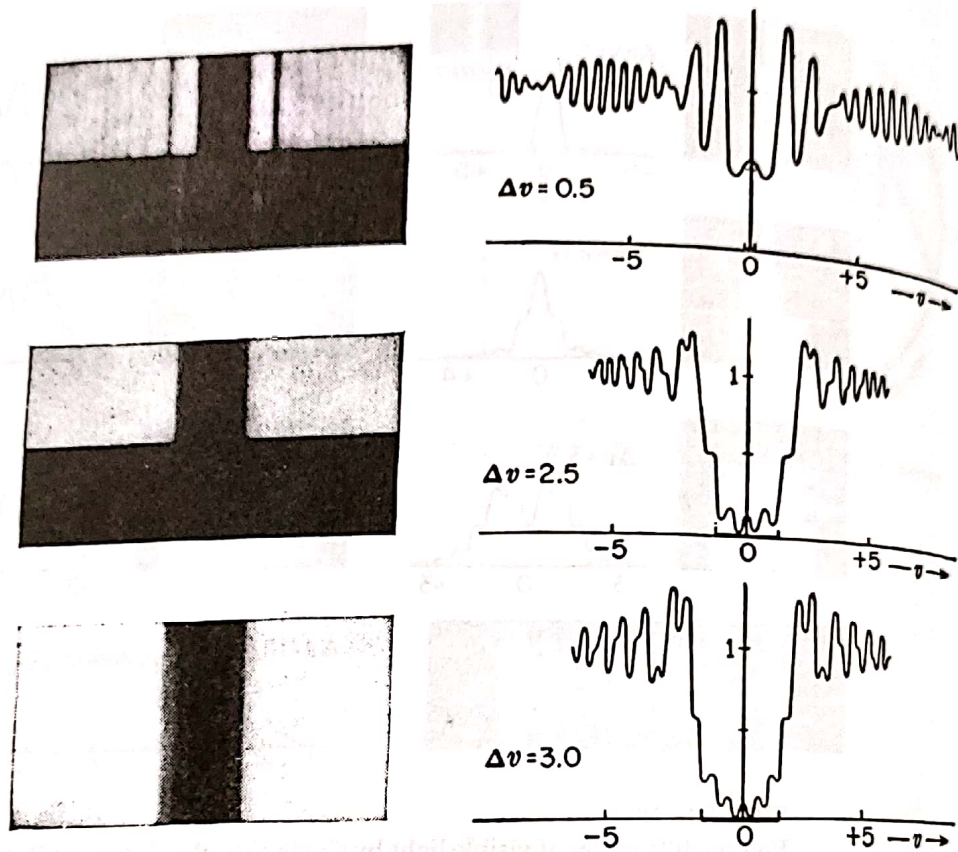


FIGURE 18V  
Fresnel diffraction by single opaque strips.

are simplified by the fact that the number of zones on one end of the interval is not limited. The values of both  $x$  and  $y$  will be  $\frac{1}{2}$  at this end. Another example of this type will now be considered.

### 8.15 DIFFRACTION BY AN OPAQUE STRIP

The shadow cast by a narrow object with parallel sides, such as a wire, can also be studied by the use of Cornu's spiral. In the case of a single slit, treated in Sec. 18.13, it was shown how the resultant diffraction pattern is obtained by sliding a fixed length of the spiral,  $\Delta v = \text{const}$ , along the spiral and measuring the chord between the two end points. The rest of the spiral out to infinity, i.e., out to  $Z$  or  $Z'$  on each side of the segment in question, was absent owing to the screening by the two sides of the slit. Now the opening of the slit in Fig. 18S(a) is replaced by an object of the same size and the slit jaws taken away, we have two segments of the spiral to consider. Suppose the obstacle is of such a size that it covers an interval  $\Delta v = 0.5$  on the spiral (Fig. 18T). At the position  $jk$  the light arriving at the screen will be due to the parts of the spiral from  $Z'$  to  $j$  and from  $k$  to  $Z$ . The resultant amplitude due to these two sections is obtained by adding their respective amplitudes as vectors. The lower section gives an amplitude represented by a straight line from  $Z'$  to  $j$ , with the arrowhead at  $j$ .

The amplitude for the upper section is represented by a straight line from  $k$  to  $Z$  with the arrowhead at  $Z$ . The vector sum of these two gives the resultant amplitude  $A$ , and  $A^2$  gives the intensity for a point  $v$  halfway between  $j$  and  $k$ . Photographs of three diffraction patterns produced by small wires are shown in Fig. 18V, accompanied by the corresponding theoretical curves.

